Supporting Information

Lytic polysaccharide monooxygenases (LPMOs) mediated production of ultra-fine cellulose nanofibres from delignified softwood fibres

Salla Koskela,[a] Shennan Wang [a], Dingfeng Xu,[a] Xuan Yang,[b] Kai Li,[a,b] Lars Berglund,[b] Lauren McKee,[a,b] Vincent Bulone[a] and Qi Zhou [a,b*]

[a] Division of Glycoscience, Department of Chemistry, KTH Royal Institute of Technology, AlbaNova University Centre, SE-106 91 Stockholm, Sweden.

[b] Wallenberg Wood Science Center, Department of Fiber and Polymer Technology, KTH Royal Institute of Technology, SE-100 44 Stockholm, Sweden.

*Corresponding author: Qi Zhou, Phone: +4687909625, e-mail: qi@kth.se

Table of Contents

Table S1. Carbohydrate composition of the original holocellulose, the control (holocellulose treated with autoclave), the nanofibres prepared by treatment with the LPMOs, NcLPMO9E and NcLPMO9F, followed by mild homogenisation.

	Arabinose (%)	Galactose (%)	Glucose (%)	Mannose (%)	Xylose (%)	Hemicellulose wt (%)		cellulose wt (%)
						glucomannan	xylan	
Original holocellulose	0.8	1.0	75.4	8.7	14.0	19.7	9.5	70.7
Control holocellulose	0.1	0.1	84.4	3.8	11.5	15.4	3.9	80.6
NcLPMO9E treated holocellulose	0.1	0.1	76.1	3.5	10.7	14.4	3.6	-
NcLPMO9F treated holocellulose	0.1	0.1	71.6	3.2	10.5	14.2	3.3	-

Table S2. Physical and average mechanical properties of the nanopapers prepared from the control holocellulose without LPMO-treatment and the LPMO-oxidised nanofibres.[a]

Material	Porosity (%)	Density (g/cm^3)	Young's modulus (GPa)	Tensile strength (MPa)	Strain-to-failure (%)	Work to fracture (MJ/m^3)
Control	7.0	1.39	12.5 (1.1)	148.7 (4.2)	2.6 (0.3)	2.2 (0.4)
NcLPMO9E	5.0	1.42	15.1 (2.3)	257.0 (6.2)	4.2 (0.7)	6.4 (0.7)
NcLPMO9F	5.7	1.41	16.3 (2.1)	262.2 (10.1)	3.7 (0.4)	6.4 (0.6)

[a] The values in parentheses are the sample standard deviations.

```
  1 GAATTCAAAA TGAGATCTAC TTTGGTTACT GGTTTGATTG CTGGTTTGTT GTCTCAACAA GCTGCTGCTC ATGCTACTTT
 81 TCAAGCTTTG TGGGTTGATG GTGCTGATTA CGGTTCTCAA TGTGCTAGAG TTCCACCTTC TAACTCTCCA GTTACTGATG
161 TTACTTCTAA CGCTATGAGA TGTAATACTG GTACTTCTCC AGTTGCTAAG AAATGTCCTG TTAAGGCTGG TTCTACTGTT
241 ACTGTTGAAA TGCATCAACA AGCTAATGAT AGATCTTGTT CTTCTGAGGC TATTGGTGGT GCTCACTACG GTCCAGTTTT
321 GGTTTATATG TCTAAGGTTT CTGATGCTGC TTCTGCTGAT GGTTCTTCTG GTTGGTTTAA AATTTTCGAA GATACTTGGG
401 CTAAGAAACC TTCTTCTTCT TCTGGAGATG ATGATTTTTG GGGTGTTAAG GATTTGAACT CTTGTTGTGG TAAAATGCAA
481 GTTAAGATCC CATCTGATAT TCCTGCTGGA GATTACTTGT TGAGAGCTGA GGTTATTGCT TTGCATACTG CTGCTTCTGC
561 TGGTGGTGCT CAATTGTACA TGACTTGTTA CCAAATCTCT GTTACTGGTG GTGGTTCTGC TACTCCAGCT ACTGTTTCTT
641 TCCCTGGTGC TTATAAATCT TCTGATCCTG GTATTTTGGT TGATATTCAC TCTGCTATGT CTACTTACGT TGCTCCAGGT
721 CCTGCTGTTT ATTCTGGTGG TTCTTCTAAG AAAGCTGGTT CTGGTTGTGT TGGTTGTGAA TCTACTTGTA AGGTTGGTTC
801 TGGTCCAACT GGTACTGCTT CTGCTGTTCC TGTTGCTTCT ACTTCTGCTG CTGCTGGTGG TGGTGGTGGT GGTGGTTCTG
881 GTGGTTGTTC TGTTGCTAAA TACCAACAAT GTGGTGGTAC TGGTTATACT GGTTGTACTT CTTGTGCTTC TGGTTCTACT
961 TGTTCTGCTG TTTCTCCACC TTACTATTCT CAATGTGTTC ATCACCACCA TCATCACTGA GCGGCCGC
```

Figure S1. Codon-optimized gene sequence for NcLPMO9E (1028 bp).

```
  1 GAATTCAAAA TGTTGCCATC TATTTCTTTG TTGTTGGCTG CTGCTTTGGG TACTTCTGCT CATTACACTT TTCCTAAAGT
 81 TTGGGCTAAC TCTGGTACTA CTGCTGATTG GCAATATGTT AGAAGAGCTG ATAACTGGCA AAACAACGGT TTCGTTGATA
161 ACGTTAATTC TCAACAAATC AGATGTTTCC AATCTACTCA TTCTCCAGCT CAATCTACTT TGTCTGTTGC TGCTGGTACT
241 ACTATTACTT ACGGTGCTGC TCCATCTGTT TATCACCCAG GTCCTATGCA ATTTTACTTG GCTAGAGTTC CTGATGGTCA
321 AGATATTAAC TCTTGGACTG GTGAAGGTGC TGTTTGGTTT AAGATCTACC ACGAGCAACC TACTTTCGGT TCTCAATTGA
401 CTTGGTCTTC TAACGGTAAA TCTTCTTTCC CAGTTAAGAT CCCTTCTTGT ATCAAGTCTG GTTCTTACTT GTTGAGAGCT
481 GAACATATTG GTTTGCACGT TGCTCAGTCT TCTGGTGCTG CTCAATTCTA CATCTCTTGT GCTCAATTGT CTATTACTGG
561 TGGTGGTTCT ACTGAGCCAG GTGCTAACTA CAAAGTTTCT TTCCCAGGTG CTTATAAGGC TTCTGATCCT GGTATTTTGA
641 TTAACATCAA CTACCCAGTT CCTACTTCTT ACAAGAATCC AGGTCCTTCT GTTTTCACTT GTCATCACCA CCATCATCAC
721 TGAGCGGCCG C
```

Figure S2. Codon-optimized gene sequence for NcLPMO9F (731 bp).

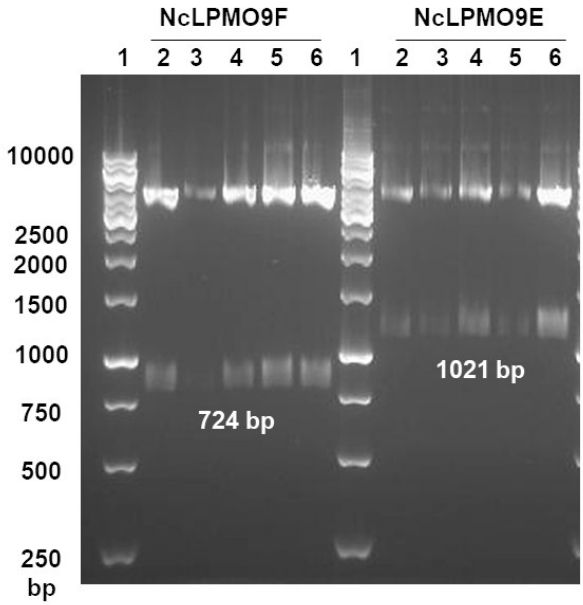

Figure S3. Restriction pattern analysis of the pPICZB vector construct containing the genes of *N. crassa* LPMOs, where lane 1=Generuler 1kb DNA ladder, Thermo Scientific (5 µL) and lanes 2-6=10 µL of the EcoRI-NotI restriction reactions.

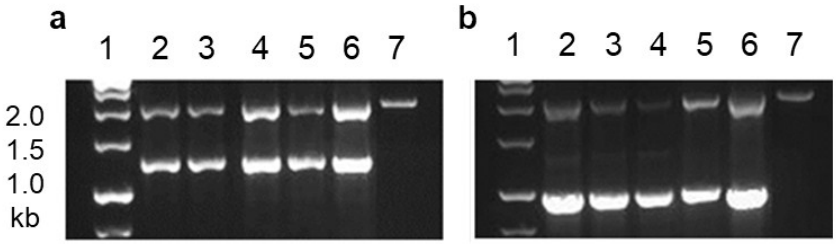

Figure S4. Colony PCR of *P. pastoris* X33 transformed with *N. crassa* LPMOs. A) NcLPMO9E, and B) NcLPMO9F, where lane 1=DNA ladder, 2-6=transformant DNA, 7=negative control untransformed *P. pastoris* X33.

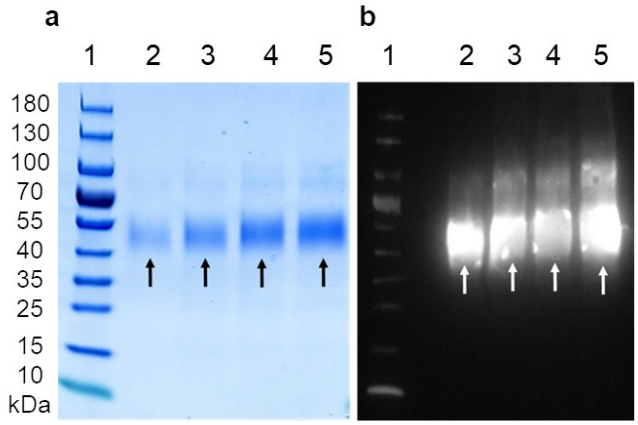

Figure S5. Production of *N. crassa* NcLPMO9E in *P. pastoris*. A) SDS-PAGE and B) western-blot, where lane 1=PageRuler prestained protein ladder (10 µL), and lanes 2-5 contain *P. pastoris* culture supernatant from 1 to 4 days of methanol induction.

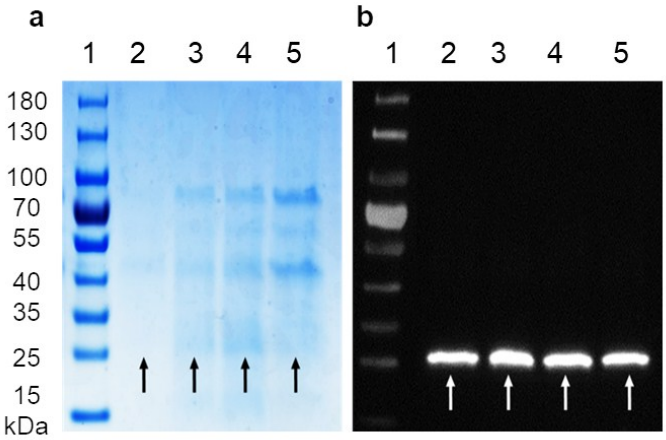

Figures S6. Production of *N. crassa* NcLPMO9F in *P. pastoris*. A) SDS-PAGE and B) western-blot, where lane 1=PageRuler prestained protein ladder (10 µL), and lanes 2-5 contain *P. pastoris* culture supernatant from 1 to 4 days of methanol induction.

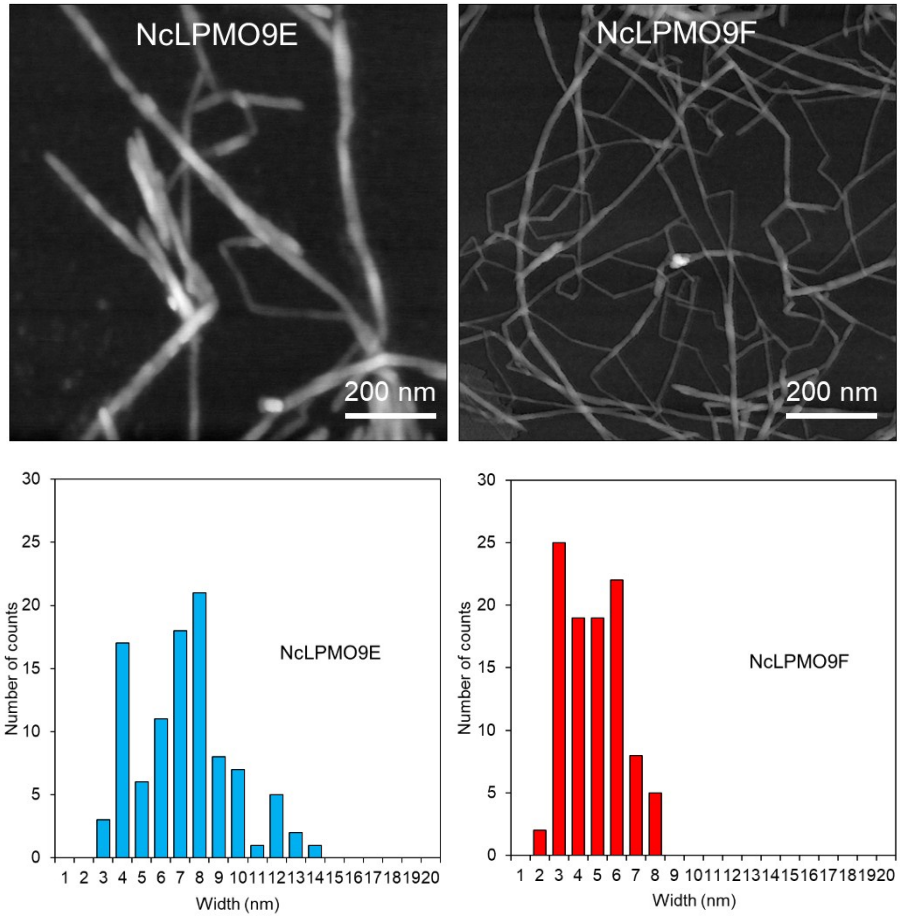

Figure S7. AFM height images and histograms showing the width distributions of CNFs produced from NcLPMO9E-oxidised and NcLPMO9F-oxidised holocellulose.